ANKLE INJURY MECHANISMS IN OFFSET CRASHES

Kennerly H. Digges and Paul G. Bedewi
FHWA/NHTSA National Crash Analysis Center
The George Washington University

Hirotoshi Ishikawa
Japan Automobile Research Institute

ABSTRACT

A significant lateral acceleration has been measured on vehicles tested in frontal offset car-to-car crashes. Typically, the lateral acceleration was about 50% of the maximum longitudinal acceleration. The maximum longitudinal acceleration occurred during the period of maximum axial loading of the lower limbs of the test dummy. It has been postulated that the footwell acceleration may be a factor in ankle injury causation. This paper uses a finite element model of the lower limbs to explore the consequence of the transverse acceleration. The finite element model of the human leg was incorporated into an existing model of a Hybrid III dummy. The Hybrid III dummy has been previously validated, using sled and crash test data. The resulting dummy model permitted a comparison of the response of a Hybrid III leg , and a human leg. The dummy model was subjected to crash acceleration environments similar to those produced in offset crashes; however, no toepan intrusion was permitted. The response of the human leg model was much different from the dummy leg model. The dummy ankle rotated to the stops of 45 degrees in dorsiflexion, and +/- 20 degrees in inversion and eversion. The human ankle produced only 20 degrees of dorsiflexion, but 30 degrees of inversion/eversion. Limitations in the Hybrid III dummy biofidelity and injury criteria make inversion and eversion ankle injuries difficult to validate experimentally. The results with the human leg model suggest that inversion/eversion ankle injuries may be induced by transverse acceleration. The population with the lowest injury tolerance may be vulnerable to these injuries, even in the absence of footwell intrusion.

UNTIL RECENTLY, injuries to the lower extremities have received less attention than the more life threatening injuries of the head and chest. While rarely fatal, these injuries can be very debilitating. Thomas and others suggest that toepan intrusion can increase the risk of ankle injuries (1995). However, Thomas found that 30% of the injuries occur without footwell intrusion. Studies of NASS data indicate that more than 50% of ankle and foot injury harm to restrained drivers occurs without any footwell intrusion (Malliaris 1995). These results suggest that factors other than intrusion may also play a

major role in foot and ankle injury causation. Other factors include: muscle tensing, inertia loads from the leg and upper body, footwell transverse acceleration; non-stable foot loading from footwear, the floor or foot pedals, and the position of the leg at the time of the impact.

An earlier analysis of frontal offset crash tests found that the vehicle footwell is subjected to a complex acceleration time history. A transverse acceleration was identified as a possible influence which contributes to inversion/eversion injuries of the ankle. The acceleration environment of the footwell during frontal offset crashes has been described in an earlier paper (Ishikawa 1996). In this earlier study, the acceleration profiles for eight car to car offset tests were analyzed. A summary of typical longitudinal and transverse accelerations of the vehicle footwell are shown in Figures 1 and 2. The tibia axial force is also shown in these figures.

Figure 1 shows typical longitudinal acceleration histories for car to car tests conducted with a driver's side 60% overlap and a 70 mph closing speed. The lateral acceleration (Figure 2) undergoes a reversal, peaking negative at about 60 ms, and positive at about 80 ms. The highest tibia axial force occurs at about the same time as the maximum negative lateral acceleration.

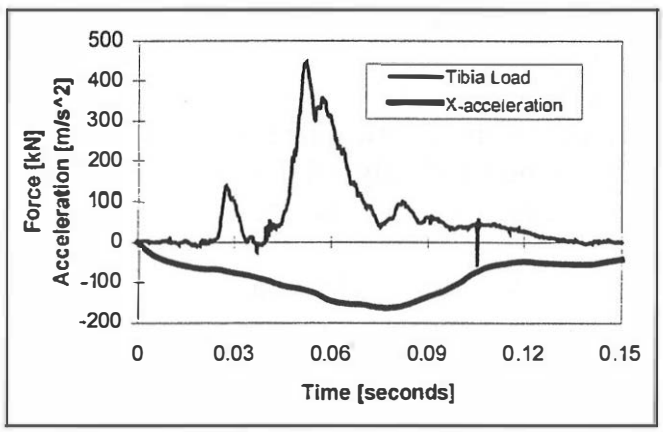

Fig. 1 - Typical foot-well longitudinal acceleration pulse for car-to-car offset collision.

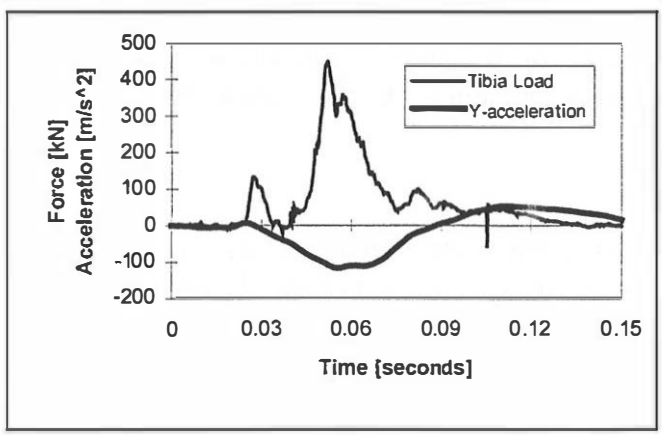

Fig. 2 - Typical foot-well longitudinal acceleration pulse for car-to-car offset collision.

In all of the tests analyzed, some footwell intrusion occurred. It has been postulated that the acceleration environments described in Figures 1 and 2 may influence ankle injuries, even in the absence of footwell intrusion. To further explore this question, a finite element model of the human leg was subjected to the acceleration environment typical of the car-to-car tests.

FINITE ELEMENT MODEL

Previous research has developed and validated a finite element model of the Hybrid III Dummy (Digges 1997). The model has been further validated for crash tests in the 1995 Ford Taurus. In this research program, the existing dummy was modified to include more detailed lower limbs. The Ford Taurus was used for the seating geometry and mechanical properties. The performance of the lower limbs was calibrated, based on crash test data.

The finite element model consists of three major components; a Hybrid III dummy, a human lower extremity, and a midsize sedan occupant compartment. The model is shown in Figure 3. The Hybrid III model of the vehicle occupant has been modified by removing the right lower extremity and replacing it with a more human-like lower limb. A more detailed description of the Hybrid III model was reported in the aforementioned study. Joint properties for the Hybrid III ankle were taken from a study performed by Crandall *et al.* for the standard Hybrid III ankle without soft-stops (1996). This ankle was chosen as a basis for validation of the model and for consistency with the Hybrid III ankle used in the experimental car-to-car and car-to-barrier tests. Previous studies have indicated some limitations to the biofidelic nature of this particular dummy ankle (Crandall 1996, Tarriere 1995, and Hagerdorn 1995). Its characteristics include hard-stops at 45° in dorsiflexion, 35° in plantarflexion, and approximately 20° in both inversion and eversion.

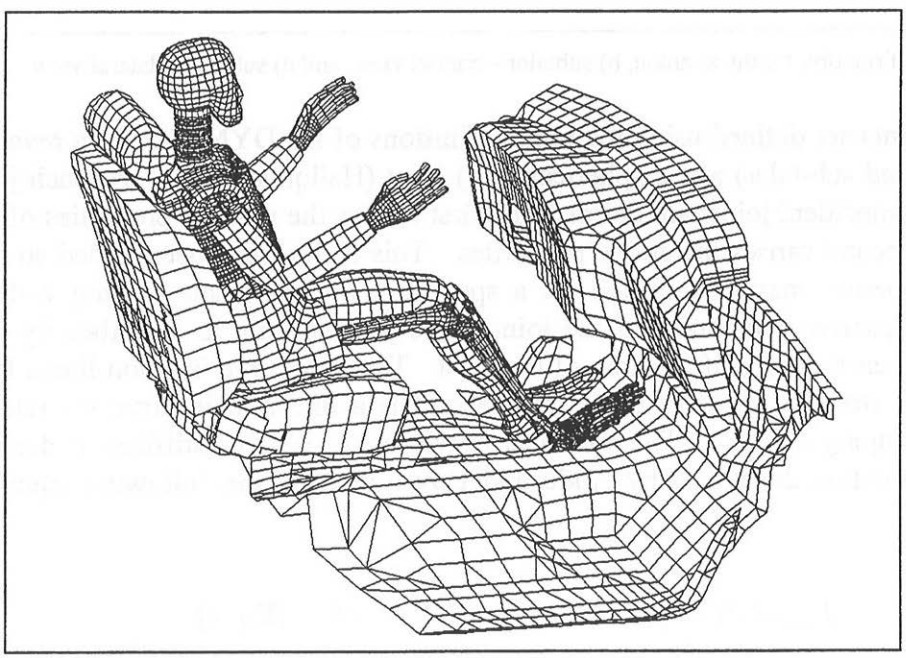

Fig. 3 - Finite element mesh of the Hybrid III dummy with human lower limb seated in a mid-size sedan.

In order to investigate the effects of the lateral acceleration pulse, a more biofidelic lower limb and ankle is desirable. For this, a human lower limb model was deemed more applicable and placed next to the Hybrid III limb for comparison. The human lower extremity model that has been developed consists of five rigid body segments connected via four joints (Bedewi 1996). The model has accurate three-dimensional geometry; however, the joints are constrained to move along a predefined axis of rotation. Figures 4 displays the axis of rotation for the ankle and subtalor joints. The focus of this model was to accurately represent the human joint characteristics for both a passive and active component of the joint. The geometry for the finite element mesh consists of the pelvis, femur, patella, tibia, fibula, and the 26 bones of the foot. The data for the geometry is of a 50th percentile male, digitized by Viewpoint Datalabs. A finite element mesh was applied to the bones and consisted of a total of 5477 thin shell elements. The mesh was then divided into five groups: the pelvis (pelvic bone), the thigh (femur), the leg (patella, tibia, and fibula), the talus, and the foot (calcaneus, cuboid, 3 cuneiforms, 5 metatarsals, navicular, and 14 phalanges). The mass, dimensions, and moments of inertia of each segment match that of a 50th percentile male as reported in various anthropomorphic studies (Robbins 1983 and McConville 1980).

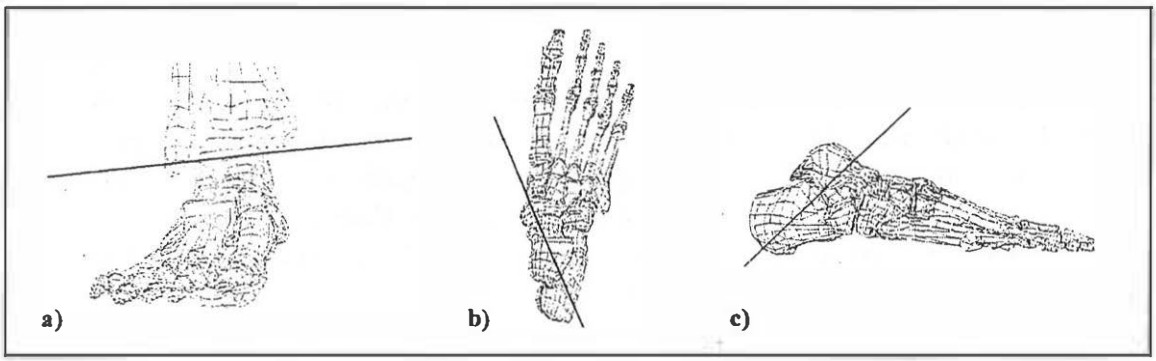

Fig. 4 - Joint axis of rotation for the a) ankle, b) subtalor - cranial view, and c) subtalor - lateral view

The joints are defined using the joint definitions of LS-DYNA3D for a revolute (knee, ankle, and sub-talar) and a spherical (hip) joint (Hallquist 1994). At each joint location, two coincident joints are defined; the first carries the passive properties of the joint and the second carries the active properties. This feature has been added so that the active properties may be adjusted for a specific level of muscle tensing without disrupting the passive component of the joint. The passive joint is described by two load curves for each degree of freedom of the joint. The first curve is a non-linear load curve for joint stiffness vs. joint angle, the second is a linear load curve for rate of rotation vs. damping moment. The nonlinear curve for the passive stiffness is derived from the formulation developed by Audu and Davi given by the following equation (1985):

$$M_{pass}(\theta,\dot{\theta}) = k_1 e^{-k_2(\theta-\theta_2)} - k_3 e^{-k_4(\theta_1-\theta)} + c\dot{\theta} \quad \text{[Eq. 1]}$$

The k values are stiffness constants and depend upon the joint being modeled, c is the passive damping constant, and the values θ_1 and θ_2 are angles approximating the joint's limit in each direction. The composition of this equation is such that, as θ reaches the joint's limit, the joint becomes extremely stiff. For joints with more than one degree-of-freedom, constants for the equation in each direction are needed. Therefore, joints such as the hip, have their passive moment described by three equations (flexion-extension, abduction-adduction, and internal-external rotation). The k and c values for Equation 1 for the joints of the lower extremity used in this model are given in Table 1. The k and c values for the lower extremity were determined experimentally by Yamaguchi (1993). The joint moment characteristics for the ankle and subtalor joints determined by Yamaguchi are consistent with values published in other studies as well (Crandall 1996 and Parenteau 1995).

Table 1 - Stiffness and damping constants for the joints of the lower extremity (units are in meters, seconds, kilograms, and radians)

Joint	Degree-of-freedom	k_1	k_2	k_3	k_4	c	θ_1	θ_2
hip	flexion-extension	2.6	5.8	8.7	1.3	1.09	1.92	-.174
hip	abduction-adduction	8.7	4.5	8.7	7.5	1.09	.506	-.710
hip	internal-external rotation	25.0	10.0	25.0	10.0	3.27	.576	-.576
knee	flexion-extension	3.1	5.9	10.5	11.8	3.17	0.00	-1.92
ankle	plantarflexion-dorsiflexion	2.0	5.0	9.0	5.0	.943	.349	-.524
sub-talar	inversion-eversion	11.5	5.0	5.5	5.0	.75	.559	-.419

Table 2 - Maximum active moment produced by muscles spanning the joints of the lower extremity.

Joint	Degree of Freedom	Maximum Active Stiffness Moment [N-m]	Active Damping Constant [kg-m/s]
hip	flexion	200	15
	extension	215	15
	adduction	200	15
	abduction	200	15
	internal rotation	200	75
	external rotation	200	75
knee	flexion	80	30
	extension	250	30
ankle	plantarflexion	180	15
	dorsiflexion	75	15
sub-talar	inversion	90	15
	eversion	50	15

The active joint is also described by two load curves in each degree of freedom. These two curves are both linear and represent the active stiffness vs. joint angle and the active rate of rotation vs. damping moment. Several load curves may be interchanged to represent different levels of muscle activation. For each joint, muscle tension can be represented by a scaled portion of 100% activation. In Table 2 the value for the maximum activation level of a joint in each degree-of-freedom is listed. The values used for maximum muscle activation are based on data collected in the open literature

(Gordon 1977 and Batman 1991). For the simulations in this study, 50% muscle activation was applied. The values for 50% activation have simply been scaled from the 100% activation values.

In total, the complete model contains 18,610 elements, many of which have been rigidized. All analysis was performed using LS-DYNA3D on two processors of a Silicon Graphics Power Challenge symmetric multi-processor supercomputer. Simulation times were approximately 8 hours per run.

SIMULATION METHOD AND MODEL CALIBRATION

The human limb was placed on the Hybrid III using a rigid body merge of the human pelvic bone to the Hybrid III right pelvis. Because this study focuses on the behavior of the lower limbs, the upper portion of the Hybrid III was rigidized for computational efficiency. The combined human-Hybrid III model was positioned in the driver side of a midsize sedan with both feet placed flat on the floor-board (Figure 5). The occupant is belted, however there is no airbag present. Most of the car-to-car test data was for belted drivers, and the air bag was considered an unnecessary complication. The geometry for the floor-board was digitized from the occupant compartment of a 1995 Ford Taurus. Material properties of sheet metal were assigned using an elastic-plastic material in LS-DYNA3D.

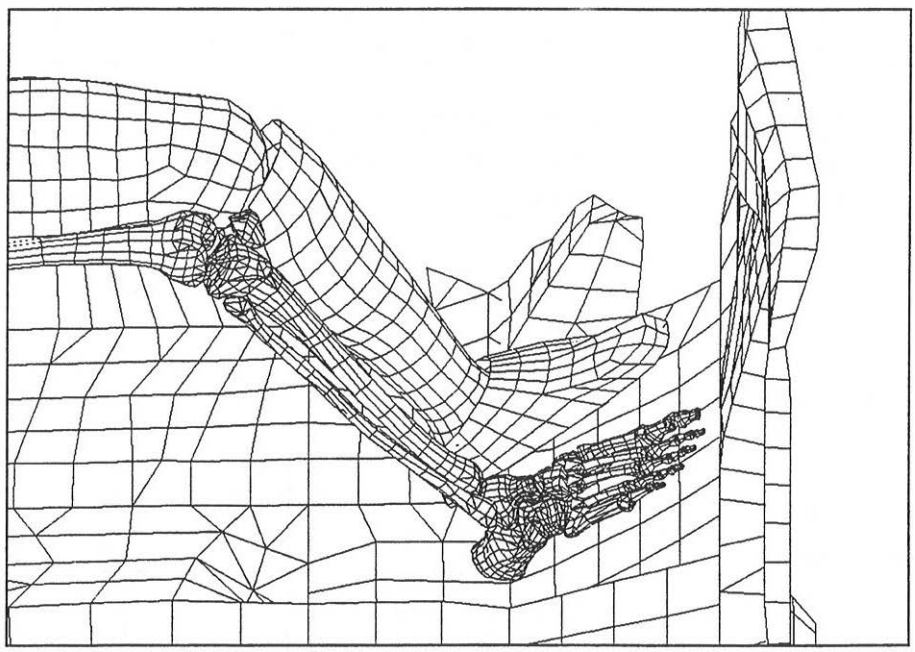

Fig. 5 - Dummy and human foot placement on the floor-board.

The average lateral and longitudinal crash pulse of the car-to-car tests was applied to the vehicle compartment. The lateral crash pulse is responsible for a relative change in position of the footwell area of approximately 100 mm to the right followed by a shift and return of 50 mm to the left over the duration of 150 ms.

A tibia load cell represented by a translational joint with linear stiffness was placed at the midpoint of both legs to measure the axial loads during the impact event. The load cell in the Hybrid III leg is the primary means for comparison between the

crash tests and the simulation due to limited instrumentation on the dummy lower limbs in the full scale tests. Figure 6 shows the comparison of the Hybrid III tibia loads from the simulation with the left tibia loads from the six vehicles in the NHTSA car-to-car tests.

Some characteristics of this crash pulse are a peak of 1-2 kN at approximately 30 ms, a large second peak of 2-7 kN between 40 and 75 ms, followed by a third peak of 0-3 kN shortly following the second peak. These peaks are representative of certain events during the crash. The first peak can be attributed to the initial contact of the foot to the floor and the inertial effects of the deceleration. The second peak is the primary loading of the tibia from the floor board during the crash. The third peak present in the experimental test is likely attributed to footwell intrusion which was present to some degree in each test. These attributes can be seen in Figure 7 for the Hybrid III left tibia load cell from NHTSA test #1676.

The tibia loading from the simulation shares similarities with the first two peaks of the experimental results. No intrusion was modeled in the simulation therefore foot entrapment or forced displacements in the floor board is not possible. This allowed a small level of rebound and foot bounce from the Hybrid III resulting in the small oscillations in the tibia force following the major loading phase. This response can be attributed to the lack of damping and compliance in the Hybrid III ankle coupled with the hard-stops in the joint. Figure 8 compares the tibia loading of the human limb with that of the Hybrid III. The increased compliance and range of motion in the human joints results in a significantly lower tibia load. Peak loading of the Hybrid III was 3.1 kN in comparison to 1.9 kN for the human. Peak loading occurred between 35 and 45 ms for each.

MODEL RESULTS

Figure 9 shows the response of the ankle model in eversion/eversion. Because the dummy ankle is on the left leg its motion is a shift from inversion to eversion while the human ankle on the right is a shift from eversion to inversion. The dummy ankle hits both of the inversion/eversion stops at +/- 20 degrees. The human leg is subjected to an inversion angle of about 30 degrees during the period of maximum tibia loading.

It is evident from the Figure 10 that the maximum dorsiflexion angle for the dummy is 45 degree - the limit for the ankle joint. In contrast, the human ankle only undergoes 15 degrees of dorsiflexion. A moderate resisting torque from muscle tensing is partially responsible for this large difference in response.

A time sequence of the human leg response is shown in Figure 11.

DISCUSSION OF RESULTS

In the offset crash environment, the Hybrid III ankle model impacted against three ankle joint stops - dorsiflexion, inversion, and eversion. In contrast, the human model, exhibited limited dorsiflexion. However, the human leg model exhibited greater in inversion and eversion angles than it is possible to measure on the Hybrid III dummy. The interpretation of dummy leg results is difficult, due to the lack of biofidelity of leg compliance and of the ankle joint response.

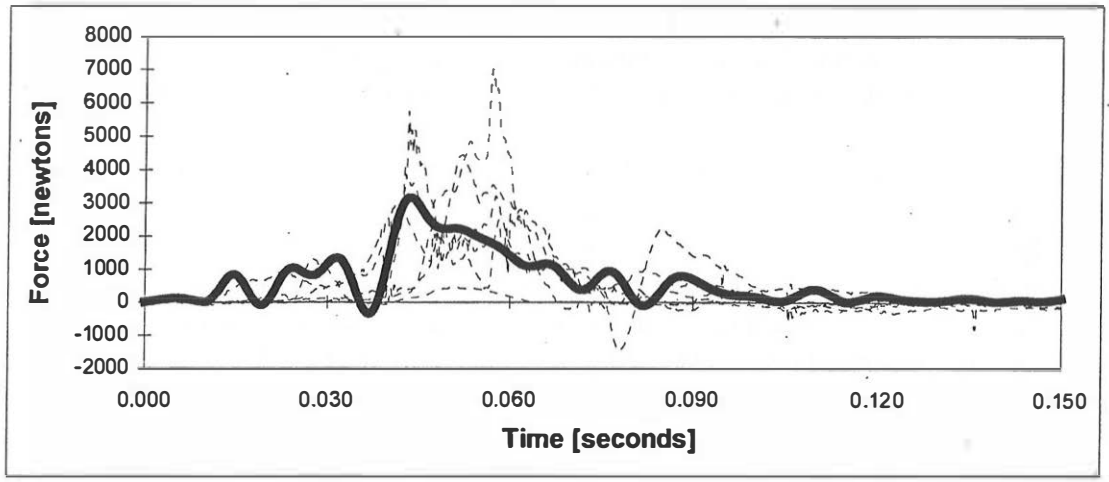

Fig. 6 - Comparison of Hybrid III left tibia load cell response from the simulation to the response obtained in the six vehicles tested by NHTSA.

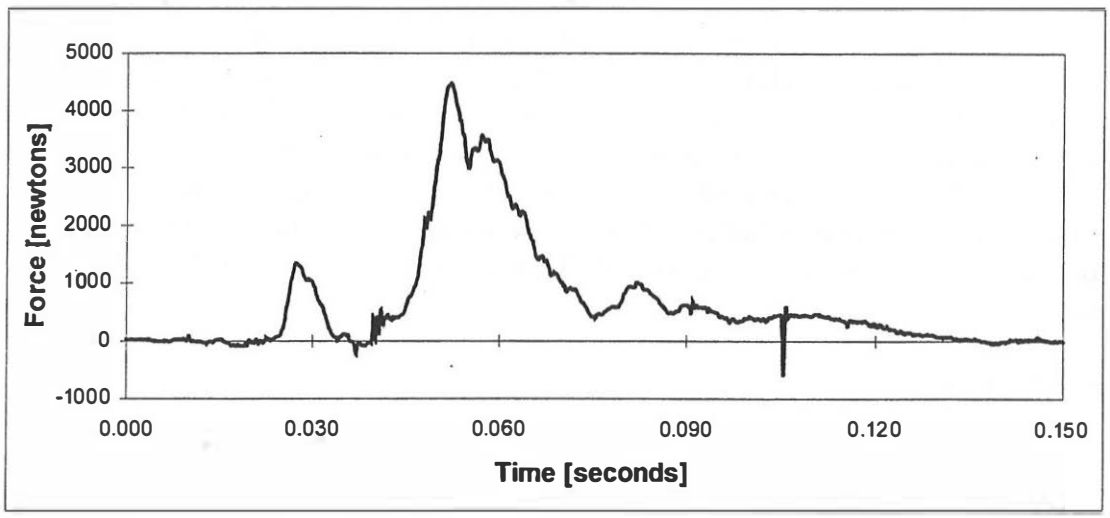

Fig. 7 - Typical Hybrid III left tibia load cell response for car-to-car frontal offset collision.

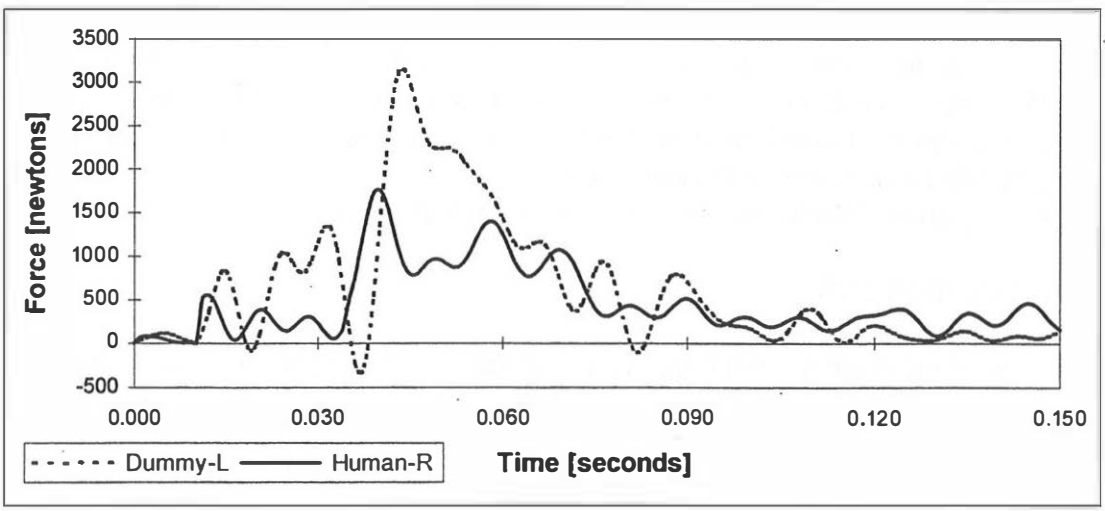

Fig. 8 - Comparison of tibia load cell response between the Hybrid III and the human obtained in the simulation.

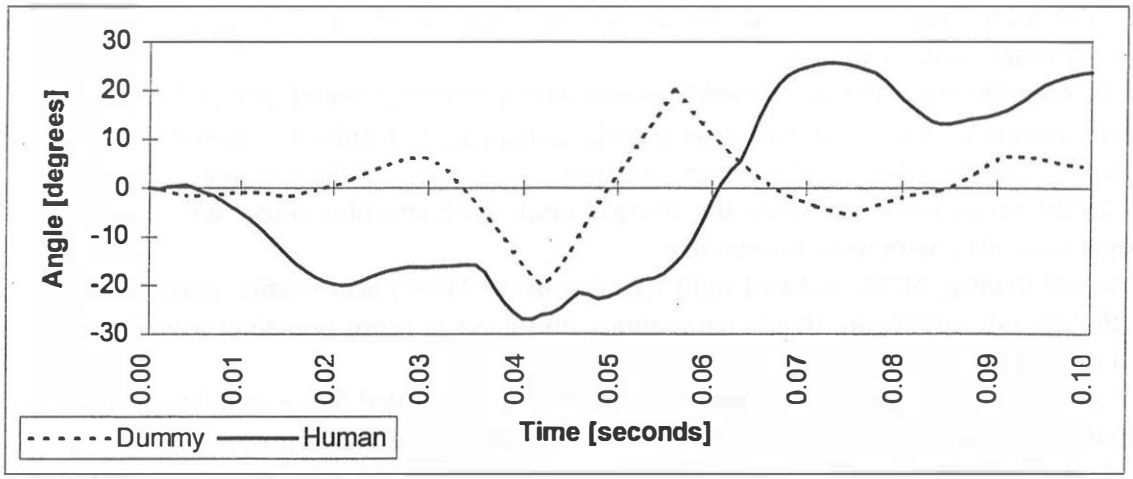

Fig. 9 - Hybrid III and human ankle response in inversion/eversion (positive angle is inversion for the human and eversion for the Hybrid III).

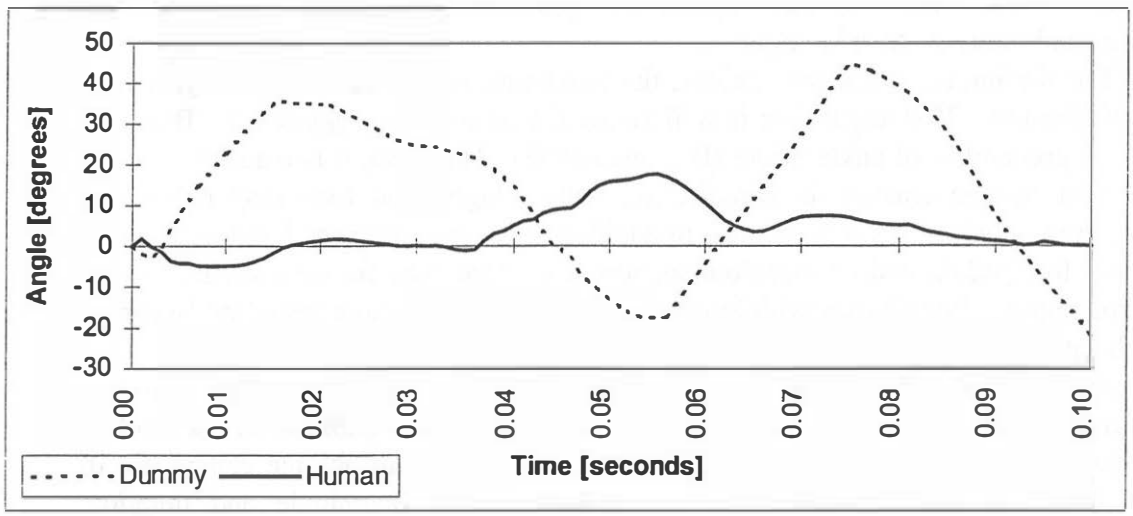

Fig. 10 - Hybrid III and human ankle response in dorsiflexion/plantarflexion (positive angle is dorsiflexion).

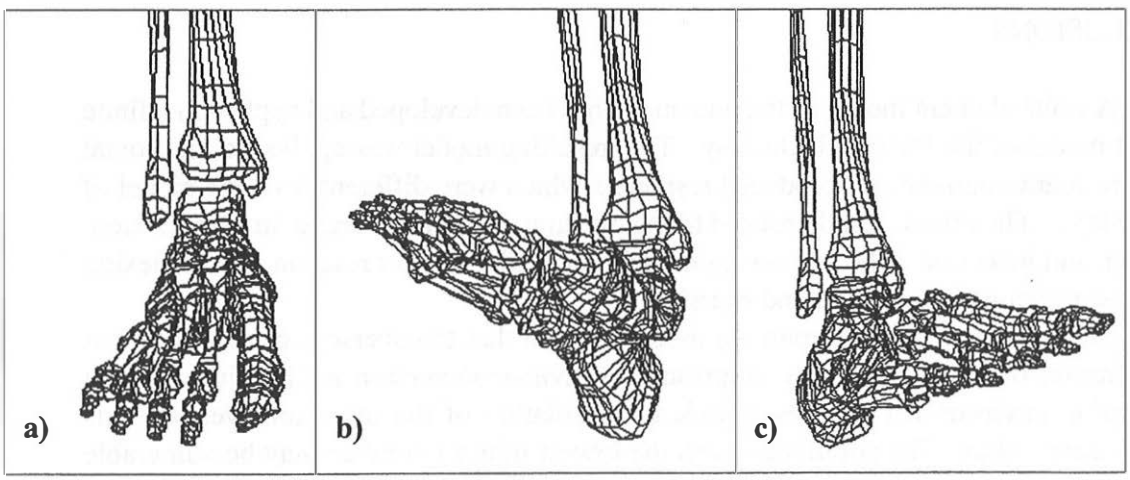

Fig. 11 - Ankle position in inversion-eversion at a) initial position at t=0 ms, b) maximum eversion of 28 at t=41 ms, and c) maximum inversion of 27 at t=74 ms.

The higher force levels and amount of dorsiflexion in the left dummy leg model can be attributed to three things:

1. More compliance in the human ankle model with a greater range of motion laterally.
2. Even small amounts of muscle tension in the human ankle results in a higher level of resistance to dorsiflexion when compared to the dummy. The human ankle is about 20 to 80 times more stiff than the dummy ankle with muscles active and 5 to 10 times more stiff with muscles inactive.
3. Unequal loading of the left and right legs due to the lateral acceleration crash pulse. Although not applicable to the simulations, intrusion is more prevalent toward the left side of the floor in the experimental tests.

A study of injured drivers treated at a hospital in the United States found that more than half of the ankle injuries occurred in frontal offset collisions. Inversion/eversion induced injuries were the most common, accounting for 60% of the ankle injuries (Lestina 1992). Studies of nationally representative accident data in the United States indicate that more than half of the injuries to the foot and ankle occur in the absence of toepan intrusion (Malliaris 1995). These results suggest that phenomena other than intrusion may contribute substantially to ankle injuries.

For the human ankle simulations, the maximum inversion/eversion angles were about 30 degrees. This angulation is well below the 60 degrees suggested by Begeman for a 50% probability of ankle injury (Begeman 1993). However, it is plausible that the presence of muscle tensing, in combination with a high axial load may reduce the angulation at which injury may occur. In addition, other environmental factors such as, footwear, foot pedals, and uneven floor support of the foot, may further contribute to the ankle angulation. Populations with injury tolerance lower that those tested by Begeman would be at greater risk.

As shown in Figures 9 and 11, the ankle undergoes angulation which is primarily in the inversion/eversion axis. The extent of this angulation is significant in the head-on car-to-car offset crashes investigated. In frontal crashes with an oblique component of impact direction, the transverse acceleration increases in magnitude and duration. Consequently, some offset crash modes not evaluated would produce even more severe acceleration environments to induce inversion/eversion angulation.

CONCLUSIONS

A finite element model of the human leg has been developed and applied to a finite element model of the Hybrid III dummy. The resulting model was applied to the frontal offset crash environment and produced responses which were different from the model of dummy leg . The dummy ankle rotated to the maximum allowable angle in dorsiflexion, inversion and inversion. The human leg model indicated a smaller rotation in dorsiflexion and larger rotations in inversion and eversion.

The results with the human leg model suggest that transverse acceleration in car to car frontal offset crashes may contribute to inversion/eversion ankle injuries. The acceleration environment induces significant angulation of the inversion/eversion axis of the human ankle. The population with the lowest injury tolerance may be vulnerable to these injuries, even in the absence of footwell intrusion. Limitations in the Hybrid III dummy lower limb biofidelity and instrumentation make inversion and eversion ankle

injuries difficult to validate experimentally. Lower limb injury criteria is needed for loading conditions of the offset crash environment.

REFERENCES

Audu, M. L., and Davy, D. T., "The Influence of Muscle Model Complexity in Musculoskeletal Motion Modeling," *Journal of Biomechanical Engineering*, (May 1985) vol. 107, no. 5, pp. 147-157.

Batman, M. and Seliktar, R., "The Effect of Muscle Contraction on the Dynamics of Car Passengers During Frontal Collision," *Advances in Bioengineering-ASME Winter Annual Meeting*, (1991) Atlanta, pp. 605-608.

Bedewi, P.G., and Bedewi, N.E., "Modelling of Occupant Biomechanics with Emphasis on the Analysis of Lower Extremity Injuries," *International Journal of Crashworthiness*, (January 1996) vol. 1, no. 1, pp. 50-72.

Begeman, P., Balakrishnan, P., Levine, R., and King, A.I., "Dynamic Human Ankle Response to Inversion and Eversion," *37th Stapp Car Crash Conference Proceedings*, (November 1993) SAE Technical Paper No. 933115.

Crandall, J.R., Hall, G.W., Bass, C.R., Klopp, G.S., Huritz, S., Pilkey, W.D., Portier, L., Petit, P., Trosseille, X., Eppinger, R.H., and Lassau, J.P., "Biomechanical Response and Physical Properties of the Leg, Foot, and Ankle," *40th Stapp Car Crash Conference Proceedings*, (November 1996) SAE Technical Paper No. 962424, pp. 173-192.

Digges, K.H., Noureddine, A., and Bedewi, N.E., "Chest Injury Risks to Drivers for Alternative Air Bag Inflation Rates," *SAE International Congress and Exposition*, (February 1997) SAE Technical Paper No. 970129.

Gordon, S. L., Orticke, P. N., Prince, J., and McMeekin, R. R., "Dynamic Characteristics of the Human Leg Joints," *Proceedings of the 21st Stapp Car Crash Conference*, (1977) SAE Technical Paper No. 770924, pp. 419-441.

Hagerdorn, A.V. and Pritz, H.B., "Development of an Advanced Dummy Leg: ALEX," *Proceedings of the First International Conference on Pelvic and Lower Extremity Injuries*, (December 1995) Washington, D.C..

Hallquist, J. O., LS-DYNA3D User's Manual: Version 930, (1994) Livermore Software Technology Corporation, Livermore, California.

Ishikawa, H. and Digges, K.H., "Vehicle Collision Force in Offset Barrier and Car-to-Car Offset Tests," *1996 International IRCOBI Conference*, (September 1996) Dublin.

Lestina, D.C., Kuhlmann, T.P., Keats, T.E., and Alley, R.M., "Mechanisms of Fracture in Ankle and Foot Injuries to Drivers in Motor Vehicle Crashes," *36th Stapp Car Crash Conference Proceedings*, (November 1992) SAE Technical Paper No. 922515.

Malliaris, A. C., "Lower Extremity Injuries In Car Crashes," FHWA/NHTSA National Crash Analysis Center Report (May 1995).

McConville, J.T., Churchill, T.D., Kaleps, I., Clauser, C.E., and Cuzzi, J., "Anthropometric Relationship of Body and Body Segments Moment of Inertia," (1980), Air Force Aerospace Medical Research Laboratory, Report No. AFAMRL-TR-80-119.

Parenteau, C. S., Foot-Ankle Injury: Epidemiology and Method to Investigate Joint Biomechanics, (1995) Thesis for the Degree of Licentiate of Engineering, Chalmers University of Technology, Gothenburg, Sweden.

Robbins, D. H., "Anthropomorphic Specifications for Mid-Sized Male Dummy," (December 1983), Transportation Research Institute Report No. UMTRI-83-53-2, United States Department of

Transportation, National Highway Traffic Safety Administration Contract No. DTNH22-80-C-07502, Washington, D.C.

Tarriere, C. and Viano, D., "Biomechanical Synthesis of New Data on Human Lower Leg Responses and Tolerances in Parallel with Dummies and Injury Criteria," *Proceedings of the First International Conference on Pelvic and Lower Extremity Injuries*, (December 1995) Washington, D.C..

Thomas, P., and Bradford, M. "A Logistic Regression Analysis Of Lower Limb Injuries," *Proceedings of the 39th Annual AAAM,* (1995), pp. 287-310.

Viewpoint Datalabs - Database Catalog, Viewpoint DataLabs, 625 South State Street, Orem, Utah, 84058, Phone 801-229-3000, FAX 801-229-3300.

Yamaguchi, G, "Kinematic Models of Joints and Musculotendon Actuation," *Movement Biomechanics* Course Notes, (1993) Arizona State University, Tempe, Arizona.